JOURNAL OF SPACECRAFT AND ROCKETS
Vol. 42, No. 6, November–December 2005

Parametric Study of Aerocapture for Missions to Venus

Scott Craig* and James Evans Lyne†
University of Tennessee, Knoxville, Tennessee 37996

A parametric study has been conducted of aerocapture for missions to Venus, examining the entry corridor width as a function of entry velocity, vehicle aerodynamics, and atmospheric density dispersions. The corridor width is found to exceed 1 deg for low lift-to-drag configurations such as an Apollo capsule. For a vehicle with a ballistic coefficient of 78 kg/m^2 and an entry speed of 12 km/s, preliminary calculations indicate that midcorridor trajectories will produce peak stagnation-point heating rates approximately 30% higher than those encountered on Apollo lunar return. Trajectories with modest deceleration loads (under 20 g) and reasonable postaerocapture propulsive requirements were readily identified. Aerocapture is found to merit further study for its potential application on future missions to Venus.

Nomenclature

A = reference area, m^2
C_D = coefficient of drag
D = drag, N
g = standard acceleration of gravity, 9.81 m/s^2
L = lift, N
m = mass, kg
q_r = stagnation-point radiative heating rate, W/cm^2
r_n = vehicle nose radius, m
V_e = atmospheric entry velocity, km/s
V_1 = freestream velocity, m/s
ΔV = impulsive velocity increment, m/s
ρ_1 = freestream density, kg/m^3

Introduction

DURING the past 30 years, several investigators have shown that the use of aerocapture could result in substantial savings in the initial weight required in low Earth orbit for both manned and robotic missions to Mars.[1–8] The technique has also been advocated for Earth return on manned Mars missions. Aerocapture must be distinguished from aerobraking; in the first technique, aerodynamic drag is used to decelerate a vehicle from a hyperbolic approach and place it into a closed orbit about the target planet. This technique has not been used to date on a space flight program. Aerobraking, on the other hand, can be used to change the orbital parameters for a vehicle already in a closed orbit. This technique has been used with great success on the Magellan mission at Venus and on the Mars Global Surveyor and Mars Odyssey missions.[9–12]

For an aerocapture mission to be successful, the vehicle must dissipate enough energy in its initial pass through the atmosphere to be captured into a planetocentric orbit without overheating or subjecting the vehicle to excessive deceleration. To accomplish this, the vehicle's atmospheric entry angle must fall within a fairly narrow range known as the entry corridor. If the angle is too shallow (less than the overshoot limit), the vehicle will fail to be captured and will continue in a heliocentric orbit; conversely, if the entry angle is too steep (greater than the undershoot limit), the vehicle will either hit the surface, overheat, or subject the crew and/or structure to excessive deceleration loads. The location and width of the entry corridor depend on the vehicle's arrival velocity V_e and aerodynamic characteristics (primarily the lift-to-drag ratio L/D and, less important, the ballistic coefficient $m/C_D A$).

Although aerocapture has been extensively studied for Mars missions,[1–8] its application at Venus has not been systematically evaluated. However, the relatively high ΔV necessary for orbital insertion make Venus aerocapture an attractive alternative and merit its evaluation.

Methodology

In this investigation, Venus aerocapture trajectories are calculated over a matrix of potential entry conditions using the three-degree-of-freedom version of the program to optimize simulated trajectories (3-D POST).[13] The entry vehicle is assumed to be a scaled-down Apollo configuration with a mass of 300 kg, a body radius of 1 m, and an effective nose radius of 1.54 m. Trajectory simulations are conducted for vehicle angles of attack of 156.7 and 166.7 deg, corresponding to lift-to-drag ratios of 0.35 and 0.2, respectively. These values of angle of attack are consistent with the original definitions used during the Apollo program, with the positive x axis defined in the direction of the pointed apex of the cone rather than in the direction of the windward, blunt face of the vehicle (Fig. 1). Entry simulations are begun at an altitude of 180 km, and this is the altitude at which entry angles are measured. A higher initial altitude is used in this study than in typical studies of Mars and Earth atmospheric entry due to the relatively higher density of the Venusian atmosphere. The vehicle is required to capture to a low, near-circular orbit with a period of approximately 92 min, an apoapse of 407 km, and a periapse of 107–112 km. In this preliminary analysis, no constraint is imposed on the final orbital inclination or the longitude of the ascending node. All entries are begun at 0° latitude, with an initial azimuth of 90 deg (due east). The entry velocities and entry angles quoted are planet-relative rather than inertial values. Atmospheric density profiles are taken from Ref. 14, and a nocturnal profile is used unless otherwise noted. Following the aerocapture, a propulsive maneuver is used to raise the periapse and place the vehicle in a 407-km, low circular orbit.

Stagnation-point convective heating rates are calculated using the methods described in Ref. 15. Radiative heating is determined using Eqs. (1–3), which were developed by Tauber based on the results of Ref. 16. These equations assume thermochemical equilibrium and give the stagnation-point, radiative heating rate as a function of the vehicle nose radius r_n, the freestream velocity V_1, and the freestream density ρ_1 for three ranges of V_1. Both the convective and radiative heating calculations ignore the effect of ablation product injection

Presented as Paper 2002-4730 at the Atmospheric Flight Mechanics Conference, Monterey, CA, 5–8 August 2002; received 21 May 2003; revision received 7 April 2004; accepted for publication 7 April 2004.

*Graduate Student, Department of Mechanical, Aerospace and Biomedical Engineering. Student Member AIAA.
†Associate Professor, Department of Mechanical, Aerospace and Biomedical Engineering. Member AIAA.

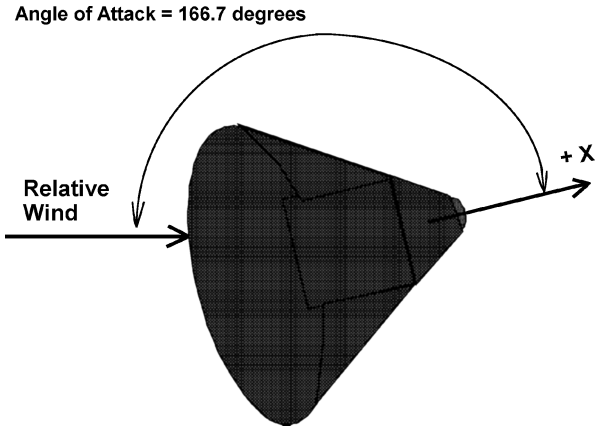

Fig. 1 Apollo configuration angle-of-attack definition.

into the shock layer:

$$\dot{q}_r = 3.07(10^{-48})V_1^{13.4}\rho_1^{1.2}r_n^{0.49} \quad \text{for} \quad 10{,}000 \le V_1 \le 12{,}000 \tag{1}$$

$$\dot{q}_r = 1.22(10^{-16})V_1^{5.5}\rho_1^{1.2}r_n^{0.49} \quad \text{for} \quad 8{,}000 \le V_1 < 10{,}000 \tag{2}$$

$$\dot{q}_r = 3.33(10^{-34})V_1^{10.0}\rho_1^{1.2}r_n^{0.49} \quad \text{for} \quad V_1 < 8{,}000 \tag{3}$$

Results

Atmospheric Trajectories

The entry corridor bounds for an L/D of 0.35 are shown in Fig. 2. The vehicle mass and reference area are 300 kg and 3.1416 m^2. Figure 2 shows undershoot boundaries calculated using various assumptions, including a case that targets only the apoapse altitude of the exit orbit (indicated in Fig. 2 as no roll), a case that targets both apoapse and periapse (at 407 and 112 km, respectively), and a case that imposes a 20-g deceleration limit, with no periapse targeting. (The 20-g limit is based on original structural design constraints from the Apollo program.[17] In the first two cases, no constraint is imposed on the vehicle deceleration.) As will be shown later, targeting both the apoapse and periapse leads to a significant reduction in the ΔV required after aerocapture for orbital circularization; however, this approach markedly reduces the entry corridor width, as does imposing a 20-g limit. Nevertheless, the total corridor equals or exceeds 1 deg at all entry speeds, even when both the periapse targeting and 20-g limit are applied. An increase of 100% in the vehicle's ballistic coefficient produces only a minimal change in the corridors shown in Fig. 2. Previous studies of aerocapture at Mars have used a corridor requirement of 1 deg to allow for uncertainties in vehicle aerodynamics and atmospheric conditions and for errors in the vehicle's atmospheric entry angle.[7,8] Application of a deceleration constraint more stringent than the 20-g limit applied here would reduce the entry corridor width from that shown in Fig. 2. If a 1-deg corridor were to be maintained over the range of potential entry speeds, this would necessitate the use of a vehicle with a higher lift-to-drag ratio.

Results obtained using daytime density profiles from Ref. 14 were virtually indistinguishable from those shown in Fig. 2 (which was calculated using the nominal nocturnal density profile). The impact of a uniform increase or decrease of 30% in atmospheric density was also investigated. A fixed, low-density profile (70% of nominal density) adversely impacts the overshoot boundary slightly, whereas a high-density profile (130% of nominal) restricts the undershoot boundary as compared to the nominal case. However, the overall reduction in corridor width resulting from a 30% uncertainty in atmospheric density appears to be less than 0.2 deg.

Figure 3 shows the corridor bounds for the vehicle at an angle of attack of 166.7 deg ($L/D = 0.2$). For the undershoot boundary with a targeted periapse, the corridor width is between 0.6 and 0.75 deg throughout Fig. 3. As would be expected, this is significantly narrower than the corridor for the higher L/D angle of attack.

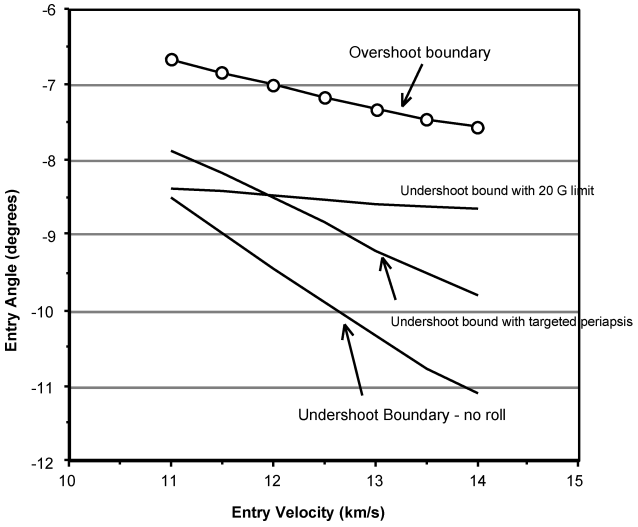

Fig. 2 Undershoot and overshoot boundaries for the aerocapture of Apollo configuration at Venus; *L/D* = 0.35.

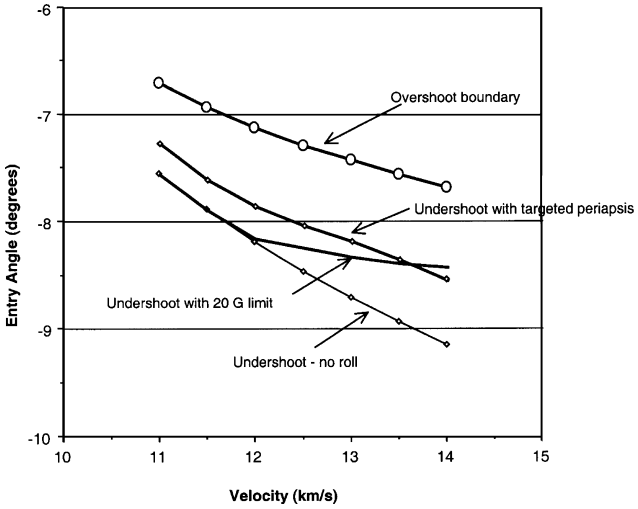

Fig. 3 Entry corridor bounds for aerocapture of an Apollo configuration at Venus; *L/D* = 0.2.

Figures 4–6 show the altitude, deceleration, dynamic pressure, and stagnation-point heating rate vs time for the same vehicle represented in Figs. 1 and 2 ($L/D = 0.35$). The atmospheric entry speed is 12 km/s, and the nocturnal atmospheric density profile is employed. Peak decelerations are seen to be reasonable, and the vehicle remains at a relatively high altitude, even for the undershoot trajectory. These high-altitude trajectories (as compared to Mars and Earth aerocapture) can be attributed to the relatively high density of the Venus atmosphere. For this case, stagnation-point heating rates do not exceed 800 W/cm^2 for the no-roll undershoot trajectory, whereas peak rates for the overshoot trajectory are approximately 150–175 W/cm^2. The heating pulse is also shown for a midcorridor trajectory, defined as having an entry angle approximately halfway between the overshoot boundary and the 20-g undershoot bound. (In this case, this puts the midcorridor entry angle at −7.79 deg.) For this trajectory, a constant bank angle was found that gave the desired target apoapse altitude. Peak heating for this midcorridor case (which is probably more representative of the nominal entry condition than either the overshoot or the undershoot heating pulse) is approximately 410 W/cm^2, compared to a peak heating rate for Apollo lunar return of about 300 W/cm^2 (Ref. 17). Integrated heat loads are 12, 15, and 29 kJ/cm^2 for the undershoot, midcorridor, and overshoot trajectories, compared to approximately 30 kJ/cm^2 for Apollo lunar return.[17]

Table 1 Postaerocapture circularization ΔV for a target orbit at 407-km altitude

Entry velocity, km/s	Overshoot trajectory, m/s	Undershoot trajectory, ms	
		No roll maneuvers/ no periapse targeting	With periapse targeting
11.0	83	324	86
11.5	83	372	84
12.0	83	427	84
12.5	83	476	84
13.0	83	535	84
13.5	83	584	99
14.0	83	649	101

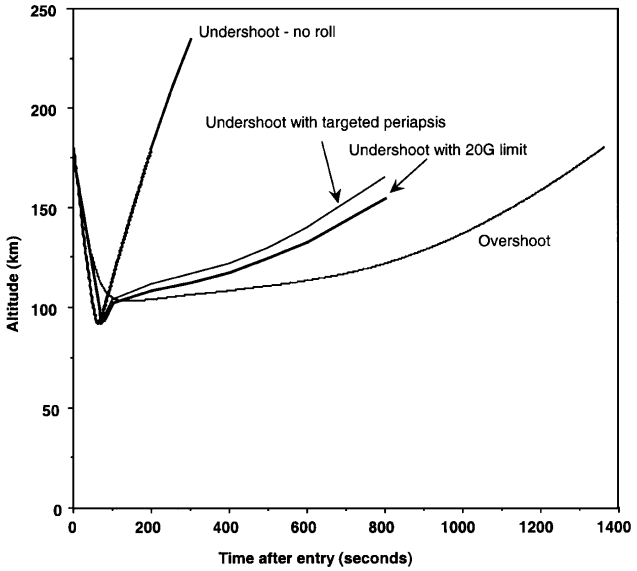

Fig. 4 Altitude histories for aerocapture of an Apollo configuration entering Venus atmosphere at 12 km/s; *L/D* = 0.35.

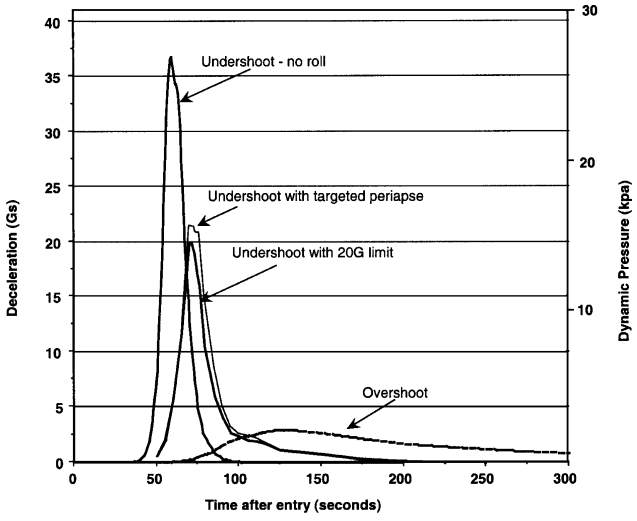

Fig. 5 Deceleration and dynamic pressure profiles for aerocapture of an Apollo configuration entering Venus atmosphere at 12 km/s; *L/D* = 0.35.

Postaerocapture Propulsive Requirements

Table 1 shows the propulsive ΔV required after the aerocapture maneuver to circularize the orbit at an altitude of 407 km. The data are presented for the overshoot trajectory and for two types of undershoot trajectory. For the case with no periapse targeting, the trajectory simulation targets only the apoapse altitude. This scheme allows steeper entries than if both apoapse and periapse are targeted, and this results in a wider entry corridor.

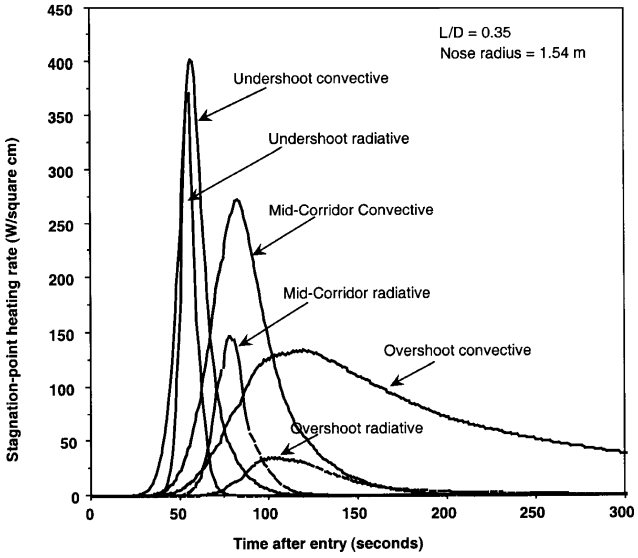

Fig. 6 Stagnation-point heating rates for aerocapture of an Apollo configuration entering Venus atmosphere at 12 km/s; *L/D* = 0.35.

However, in these trajectories, the vehicle exits the atmosphere with a steeper flight path, and the resulting orbit has a lower periapse, thereby requiring a much larger propulsive expenditure for circularization.

If a specific impulse of 320 s is assumed (typical for a storable propellant), less than 10 kg of propellant is required for circularization for the overshoot cases and for the undershoot trajectories that employ periapse targeting. However, postaerocapture propellant requirements can exceed 50 kg (of the total vehicle mass of 300 kg) for the undershoot trajectories that do not use periapse targeting.

Conclusions

The present study examines the feasibility of using aerocapture for orbital insertion at Venus. Entry corridor width is determined as a function of atmospheric entry velocity, aerodynamic heating rates and integrated heat loads are calculated, and postaerocapture ΔV is investigated.

An Apollo-style capsule with an L/D of 0.35 is found to provide corridor widths of at least 1 deg throughout the range of potential entry speeds, while limiting the vehicle's deceleration to less than 20 g. These corridor widths satisfy criteria adopted in previous studies of aerocapture for Mars missions. Postaerocapture ΔV is found to be modest, requiring as little as 10 kg of propellant to trim the orbit of a 300-kg capsule. A vehicle entering the atmosphere at 12 km/s and flying a midcorridor trajectory experiences a peak heating rate of approximately 410 W/cm^2 and an integrated heat load of 15 kJ/cm^2 at the stagnation point. These values compare favorably with the 300-W/cm^2 peak rate and 30-kJ/cm^2 integrated heat load encountered at the stagnation point during Apollo lunar return.

Future studies should include an evaluation of the influence of target orbit selection on the entry corridor, aerodynamic heating, and postaerocapture ΔV. Heating distributions should be calculated, and

thermal protection system must be completed to allow a comparison of aerocapture with propulsive orbital insertion in terms of overall system mass.

References

[1]Tauber, M. E., Bowles, J. V., and Yang, L., "Use of Atmospheric Braking During Mars Missions," *Journal of Spacecraft and Rockets*, Vol. 27, No. 5, 1990, pp. 514–521.

[2]Cruz, M. I., "The Aerocapture Vehicle Mission Design Concept—Aerodynamically Controlled Capture of Payload into Mars Orbit," AIAA Paper 79-0893, May 1979.

[3]Walberg, G. D., "A Review of Aerobraking for Mars Missions," International Astronautical Federation, IAF Paper 88-196, Oct. 1988.

[4]Braun, R. D., Powell, R. W., and Hartung, L. C., "The Effect of Interplanetary Trajectory Options on a Manned Mars Aerobrake Configuration," NASA TP-3019, Aug. 1990.

[5]Wilcockson, W. H., "L/D Requirements for Mars Aerocapture Missions," AIAA Paper 90-2937, Aug. 1990.

[6]Lyne, J. E., and Braun, R. D., "Flexible Strategies for Manned Mars Missions Using Aerobraking and Nuclear Thermal Propulsion," *Journal of the Astronautical Sciences*, Vol. 41, No. 3, 1993, pp. 339–348.

[7]Lyne, J. E., Anagnost, A., and Tauber, M. E., "Parametric Study of Manned Aerocapture, Part 2: Mars Entry," *Journal of Spacecraft and Rockets*, Vol. 29, No. 6, 1992, pp. 814–819.

[8]Braun, R. D., Powell, R., and Lyne, J. E., "Earth Aerobraking Strategies for Manned Return from Mars," *Journal of Spacecraft and Rockets*, Vol. 29, No. 3, 1992, pp. 297–304.

[9]Curtis, H., "Magellan Aerobraking at Venus," *Aerospace America*, Vol. 32, No. 1, 1994, pp. 32–41.

[10]Lyons, D. T., "Aerobraking Magellan: Plan Versus Reality," American Astronautical Society/AIAA Spaceflight Mechanics Meeting, AAS Paper 94-118, Feb. 1994.

[11]Lyons, D. T., Beerer, J. G., Esposito, P. B., Johnston, M. D., and Wilcockson, W. H., "Mars Global Surveyor: Aerobraking Mission Overview," *Journal of Spacecraft and Rockets*, Vol. 36, No. 3, 1999, pp. 307–313.

[12]Lyons, D., "Aerobraking at Venus and Mars: A Comparison of the Magellan and Mars Global Surveyor Aerobraking Phases," AIAA/American Astronautical Society Astrodynamics Specialist Conf., AAS Paper 99-358, Aug. 1999.

[13]Brauer, G. L., Cornick, D. E., and Stevenson, R., "Capabilities and Applications of the Program to Optimize Simulated Trajectories (POST)," NASA CR-2770, Feb. 1977.

[14]Hunten, D. M., Colin, L., Donahue T. M., and Moroz, V. I., *Venus*, Univ. of Arizona Press, Tucson, AZ, 1983, pp. 1046–1048.

[15]Tauber, M. E., Bowles, J. V., and Yang, L., "Atmospheric Environment During Maneuvering Descent from Martian Orbit," *Journal of Spacecraft and Rockets*, Vol. 26, No. 5, 1989, pp. 330–337.

[16]Page, W. A., and Woodward, H. T., "Radiative and Convective Heating During Venus Entry," *AIAA Journal*, Vol. 10, No. 10, 1972, pp. 1379–1381.

[17]Pavlosky, J. E., and St. Leger, L. G., "Apollo Experience Report—Thermal Protection Subsystem," NASA TN D-7564, Jan. 1974.

C. Kluever
Associate Editor